Meteorological and Microphysical Controls on the Stratocumulus to Cumulus Transition

Johannes Mohrmann and Isabel L. McCoy
University of Washington Department of Atmospheric Sciences

Summary

- Geostationary satellite cloud observations and meteorological reanalysis are combined with air parcel trajectories to create a large **Lagrangian dataset for investigating marine boundary layer cloud evolution.**
- Spatial correlations of seasonal mean quantities show that EIS (estimated inversion strength) and to a lesser extent N_d (cloud droplet number concentration) are closely related to cloud fraction
- Composite trajectories show the expected declines in EIS, cloud fraction, and N_d.
- Correlations found when comparing across trajectories were weak or opposite to expected, with higher EIS and N_d anomalies correlating with larger changes in cloud fraction.

Motivation and Background

- Subtropical marine cloud evolution (in particular the transition of boundary layer (BL) clouds from stratocumulus to cumulus) is thought to be primarily controlled by the lower tropospheric stability[5,8,10], which can also be quantified using the **estimated inversion strength (EIS)**[9].
- Microphysical cloud properties, namely the **cloud droplet number concentration (N_d)**, may play a secondary role in affecting cloud evolution[2,7,11], though with no consensus on the direction of this effect
- While a Lagrangian perspective is preferred to capture cloud evolution, previous observational studies have been limited by data scarcity in the remote marine BL.
- Observations made during the **Cloud Systems Evolution in the Trades (CSET)** field campaign provide a much larger than previously available dataset for exploring Lagrangian cloud evolution.

Data

CSET

- Campaign took place July/August 2015
- Flights made with the NSF/NCAR Gulfstream V collected in-situ BL cloud property data in the Northeast Pacific (NEP)
- Data from cloud probes were used to validate satellite retrievals of N_d products (Figure 1)

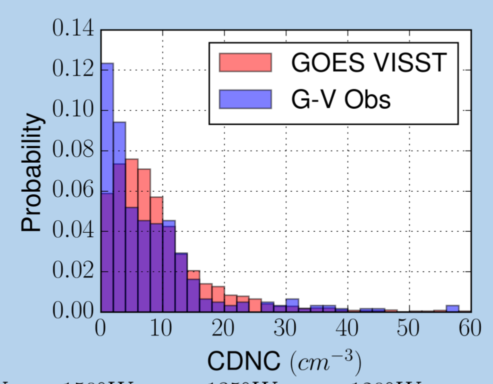

Figure 1: Histogram of N_d from aircraft observations and satellite retrievals, CSET RF07

GOES VISST Retrievals

- Satellite based retrievals of cloud properties using the VISST (Visible Infrared Solar-Infrared Split Window Technique) algorithm and GOES (Geostationary Operational Environmental Satellite) measurements were provided hourly for the duration of CSET (two months)[3,4], including cloud fraction (CF), cloud top height (CTH), and N_d (Figure 2 shows an example); certain retrievals were daytime only.

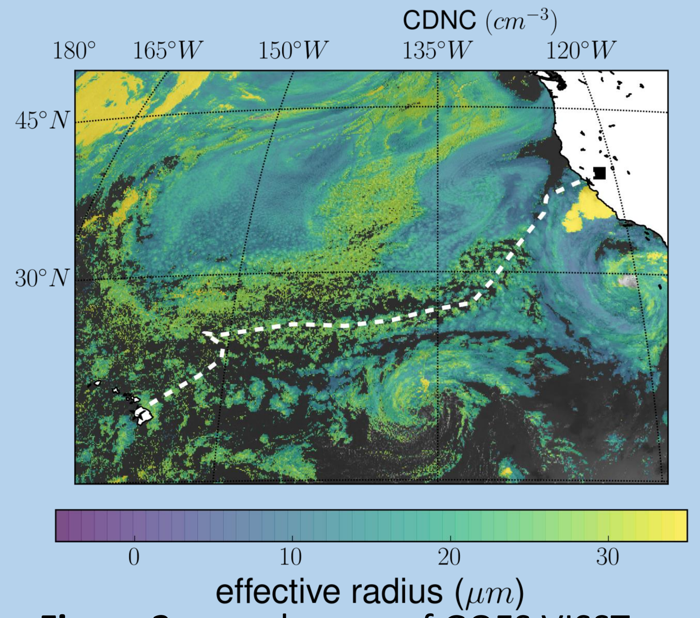

Figure 2: sample map of GOES VISST retrievals. Dashed line marks CSET RF07

Trajectories

- BL air parcel trajectories were generated using the HYSPLIT model and NCEP GDAS analysis winds
- 30 starting locations in NEP stratocumulus region, initialized every day at 0z (midafternoon local time)
- Trajectories initialized at 500m and run forward isobarically for 3 days
- Trajectories filtered by direction to head approximately southwest, resulting in 903 trajectories used in analysis

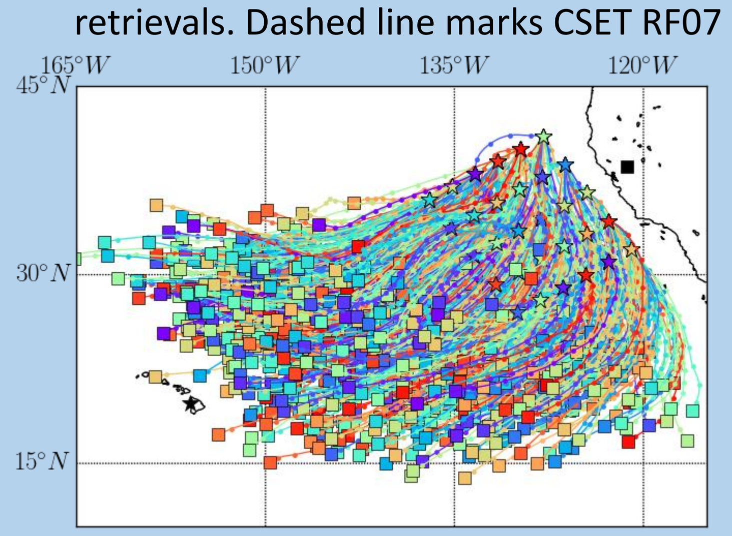

Figure 3: 903 trajectories used. Stars mark start, squares mark end

ERA-Interim

- EIS is derived from 6-hourly reanalysis meteorology using the formula $EIS = LTS - \Gamma_m^{850}(z_{700} - LCL)$[9], and in the subtropics behaves similarly to LTS

Seasonal Means

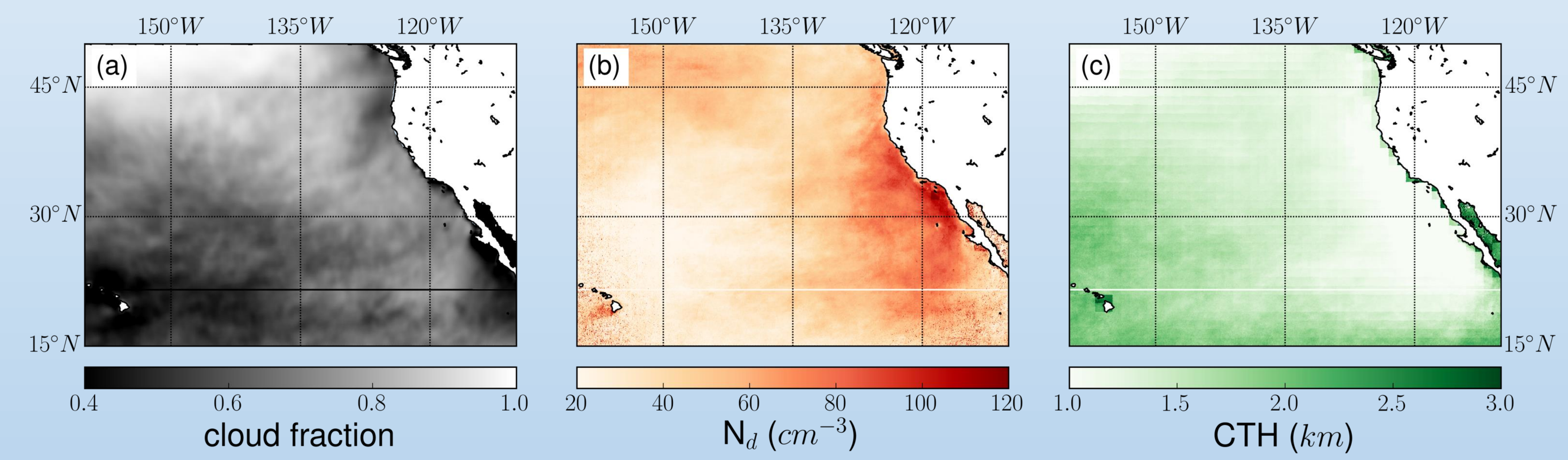

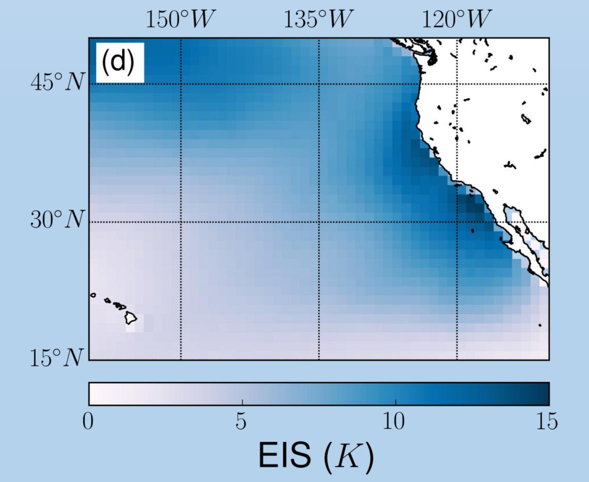

Figure 4: Mean values over July/August 2015 of (a) cloud fraction, (b) cloud droplet number concentration (c) cloud top height, and (d) estimated inversion strength. (a, b, c) are from GOES VISST, (d) is from ERA-Interim

r	N_d	EIS
CF	0.31	0.74
CTH	-0.62	-0.85

Table 1: Spatial correlations between variables from seasonal means. Consistent with existing literature[2,9,10,11]

Mean Trajectory Behavior

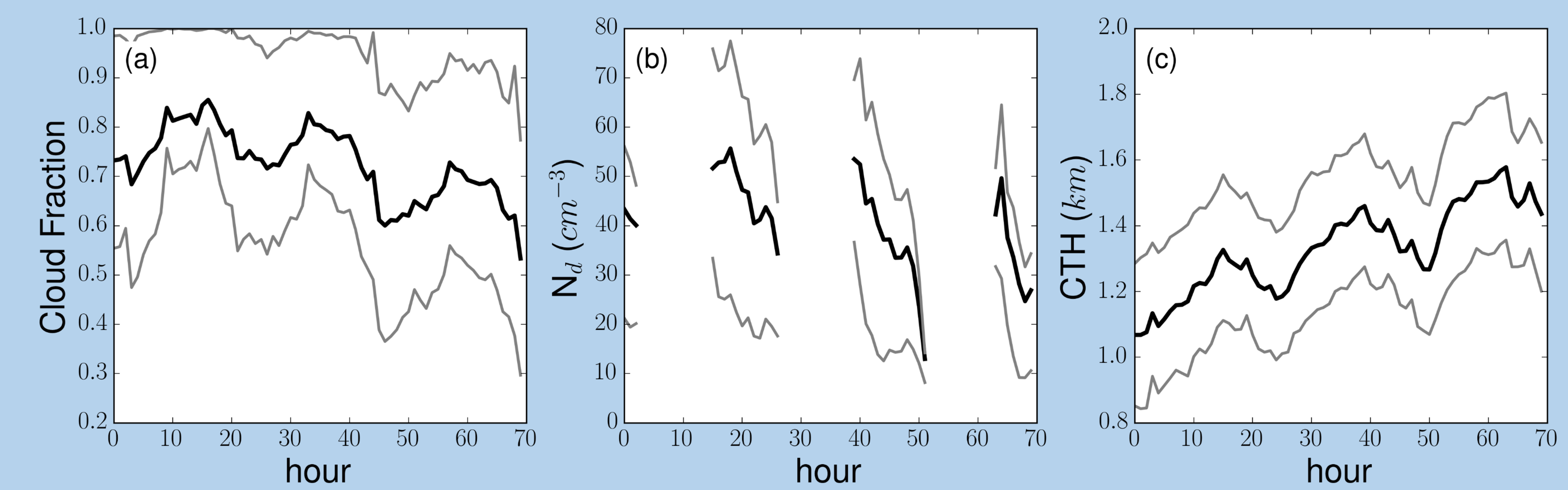

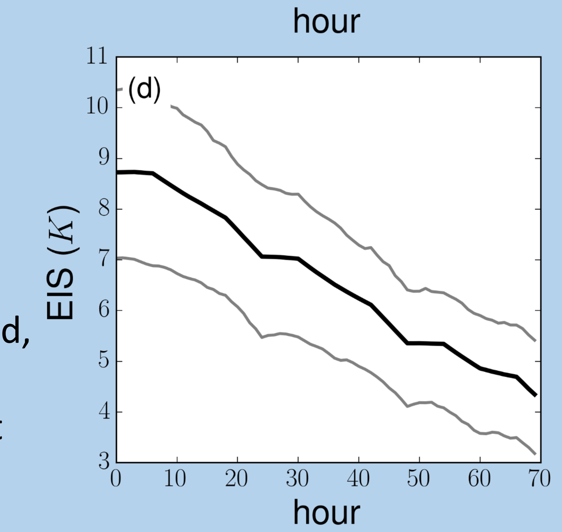

Figure 5: Mean (black) and 25th- and 75th-quartiles (grey) of trajectory evolution: (a) cloud fraction, (b) cloud droplet number concentration, (c) cloud top height, and (d) estimated inversion strength. Note that N_d is daytime only

- Mean behavior is as expected: deepening and breakup of cloud, and declining N_d with decreasing EIS along the trajectory[10,11]
- Strong diurnal signal in mean trajectory CF and CTH consistent with night-time deepening and infilling[6]

Changes in CF and N_d

- Strong correlation (r=0.5) was found between the decrease in CF and decrease in N_d.
- Decreases in N_d and CF are linear when considering mean behavior, though some trajectories show large decreases in N_d with no change in CF, followed by a large decline in CF with relatively constant N_d (not shown)

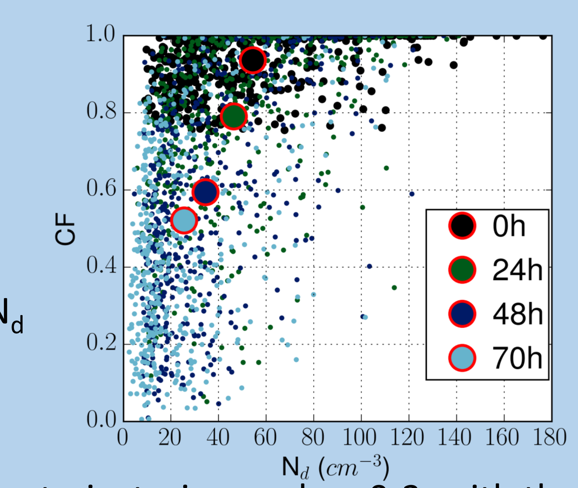

Figure 6: evolution of trajectories in CF-N_d space. Colors show trajectories on days 0-3, with the mean evolution shown in large red-circled dots. Filtered for trajectories starting with CF>0.8

Inter-Trajectory Correlations

- If cloud evolution along a trajectory (as measured by changes in CF or CTH), is controlled by EIS or N_d, we expect a correlation between EIS/N_d and CTH/CF changes. **We only find a correlation for CF and N_d** (Figure 7; negative Δ means CF decrease).
- We refine our analysis by considering changes in anomalies of CF/CTH by subtracting seasonal mean values at each location. This controls for variations in trajectory length and start location (Figure 8).
- Correlations exist between anomalies sampled at points along trajectories (not considering Lagrangian changes), particularly for N_d and CF (Figure 10).
- As a final refinement we consider residual changes in anomalies. After accounting for red noise effects, as we expect all anomalies to decay to zero. Following Eastman et al. (2016), we remove the predicted change in anomaly given the initial anomaly. **We still find only weak anticorrelations between residual CF change and EIS/N_d anomalies** (Figure 9).

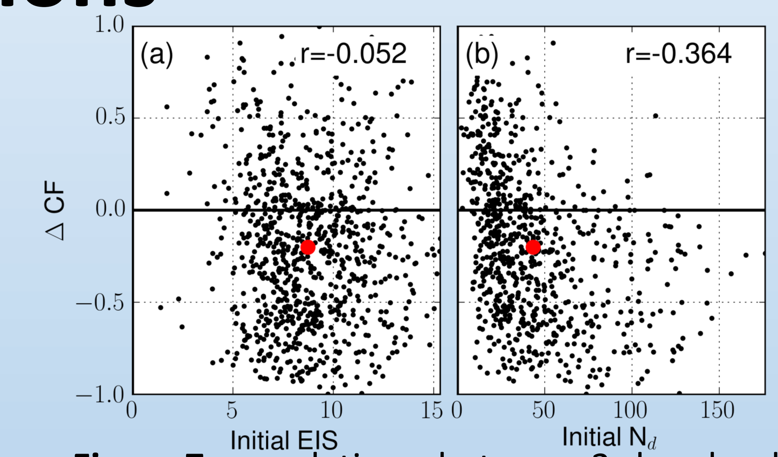

Figure 7: correlations between 3-day cloud fraction change and trajectory starting EIS (a) and N_d (b). Red dot marks centroid

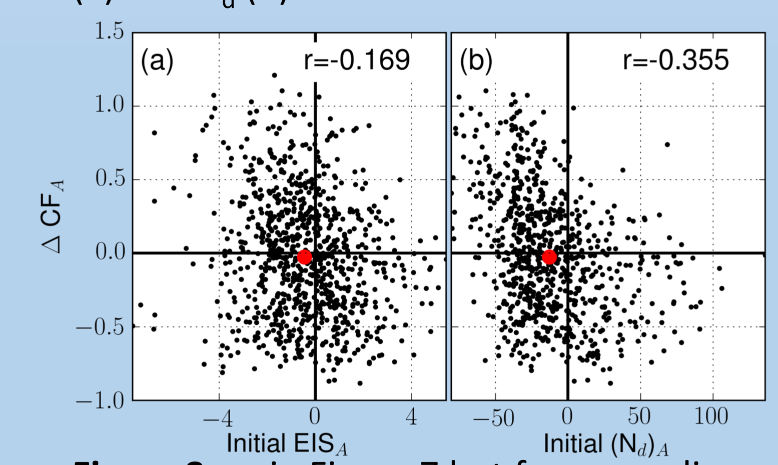

Figure 8: as in Figure 7 but for anomalies

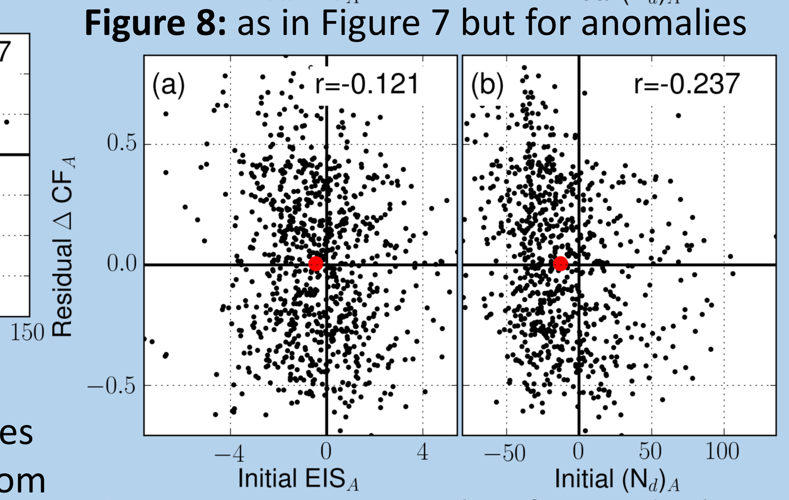

Figure 9: as in Figure 8 but for residual cloud fraction anomaly change

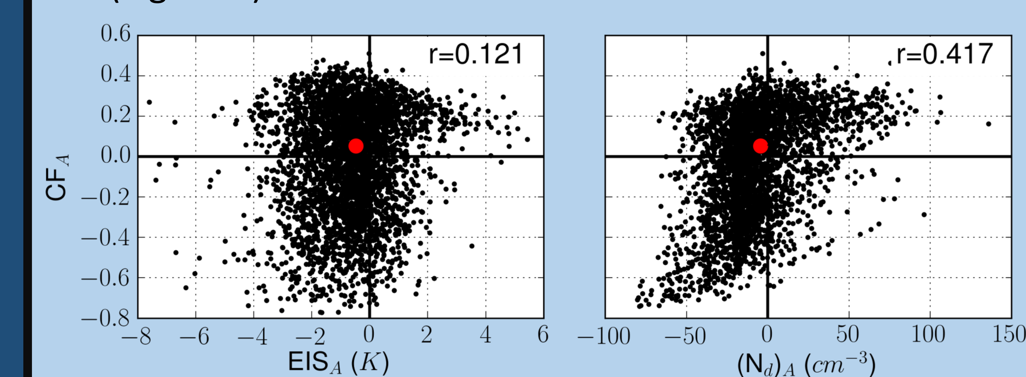

Figure 10: correlations between cloud fraction anomalies and EIS anomalies (a) and N_d anomalies (b), sampled from trajectories once per day (4 points per trajectory)

Future Work

- Consider confounding variables (e.g. free-tropospheric humidity and liquid water path) that may mask effects of stability
- Include alternative controlling variables (e.g. sea surface temperature) in analysis
- Further investigate potential nonlinear evolution of CF and N_d[2,11]

References, Acknowledgments, Contact:

Johannes Mohrmann, jkcm@uw.edu

We gratefully acknowledge Patrick Minnis (NASA LaRC) and Rabindra Palikonda (SSAI) for the provision of GOES cloud products (http://satcorps.larc.nasa.gov/CSET), the NOAA Air Resources Laboratory (ARL) (for HYSPLIT and ARL-packed NCEP GDAS datasets), the European Center for Medium-Range Weather Forecasts (ERA-Interim), and the NCAR Earth Observing Laboratory and Research Aviation Facility CSET teams. This work was supported by NSF **AGS-1445813** (J Mohrmann) and NFS GRFP **DGE-1256082** (I McCoy)

1. Eastman, Ryan, and Robert Wood. 2016. "Factors Controlling Low-Cloud Evolution over the Eastern Subtropical Oceans: A Lagrangian Perspective Using the A-Train Satellites." *Journal of the Atmospheric Sciences* 73 (1): 331–51. doi:10.1175/JAS-D-15-0193.1.
2. Jiang, Hongli. 2002. "Simulations of Aerosol-Cloud-Dynamical Feedbacks Resulting from Entrainment of Aerosol into the Marine Boundary Layer during the Atlantic Stratocumulus Transition Experiment." *Journal of Geophysical Research* 107 (D24): 4813. doi:10.1029/2001JD001502.
3. Minnis, P., L. Nguyen, R. Palikonda, et al., 2008: Near-real time cloud retrievals from operational and research meteorological satellites. Proc. SPIE Remote Sens. Clouds Atmos. XIII, Cardiff, Wales, UK, 15-18 September, 7107-2, 8 pp., ISBN: 9780819473387.
4. Palikonda, R., P. Minnis, et al., 2017: SatCORPS near-realtime global geostationary satellite-based cloud, surface temperature, radiation, and marine aerosol product suite for assimilation and nowcasting. AMS 21st Conf. Integ. Observing Assimilation Systems for Atmos, Ocean, and Land Surf., Seattle, WA, 23-26 January, 1258.
5. Pincus, Robert, Marcia B. Baker, and Christopher S. Bretherton. 1997. "What Controls Stratocumulus Radiative Properties? Lagrangian Observations of Cloud Evolution." *Journal of the Atmospheric Sciences* 54 (17): 2215–36. doi:10.1175/1520-0469(1997)054<2215:WCSRPL>2.0.CO;2.
6. Rozendaal, Margaret A., Conway B. Leovy, and Stephen A. Klein. 1995. "An Observational Study of Diurnal Variations of Marine Stratiform Cloud." *Journal of Climate* 8 (7): 1795–1809. doi:10.1175/1520-0442(1995)008<1795:AOSODV>2.0.CO;2.
7. Sandu, Irina, and Bjorn Stevens. 2011. "On the Factors Modulating the Stratocumulus to Cumulus Transitions." *Journal of the Atmospheric Sciences* 68 (9): 1865–81. doi:10.1175/2011JAS3614.1.
8. Sandu, Irina, Bjorn Stevens, and R. Pincus. 2010. "On the Transitions in Marine Boundary Layer Cloudiness." *Atmospheric Chemistry and Physics*, 2377–91. http://www.atmos-chem-phys.net/10/2377/.
9. Wood, Robert, and Christopher S. Bretherton. 2006. "On the Relationship between Stratiform Low Cloud Cover and Lower-Tropospheric Stability." *Journal of Climate* 19 (24): 6425–32. doi:10.1175/JCLI3988.1.
10. Wyant, Matthew, and Christopher S. Bretherton. 1997. "Numerical Simulations and a Conceptual Model of the Stratocumulus to Trade Cumulus Transition." *Journal of the Atmospheric Sciences*, 168–92. http://journals.ametsoc.org/doi/abs/10.1175/1520-0469(1997)054%253C0168%253ANSAACM%253E2.0.CO%253B2.
11. Xue, Huiwen, and Graham Feingold. 2006. "Large-Eddy Simulations of Trade Wind Cumuli: Investigation of Aerosol Indirect Effects." *Journal of the Atmospheric Sciences* 63 (6): 1605–22. doi:10.1175/JAS3706.1.